

Electromagnetic form factors of baryons in an algebraic approach

R. Bijker

Instituto de Ciencias Nucleares, Universidad Nacional Autónoma de México, A.P. 70-543, 04510 México D.F., México

A. Leviatan

Racah Institute of Physics, The Hebrew University, Jerusalem 91904, Israel

We present a simultaneous analysis of elastic and transition form factors of the nucleon. The calculations are performed in the framework of an algebraic model of baryons. Effects of meson cloud couplings are considered.

Key words: Baryon spectroscopy; electromagnetic form factors; algebraic methods; vector meson dominance.

Se presenta un análisis de los factores de forma electromagnéticos del nucleón en el contexto de un modelo algebraico. Se considere los efectos de los acoplamientos con la nube mesónica.

Descriptores: Espectroscopía bariónica; factores de forma electromagnéticos; métodos algebraicos; dominancia de mesones vectoriales.

PACS number(s): 13.40.Gp, 14.20.Dh, 14.20.Gk, 11.30.Na

I. INTRODUCTION

The electromagnetic form factors of the nucleon and its excitations (baryon resonances) provide a powerful tool to investigate the structure of the nucleon [1]. These form factors can be measured in electroproduction as a function of the four-momentum squared $q^2 = -Q^2$ of the virtual photon.

The elastic form factors of the nucleon have mostly been determined with the Rosenbluth separation technique. However, for values of Q^2 above a few $(\text{GeV}/c)^2$ it becomes increasingly difficult to extract the electric form factor G_E because the measured cross section is dominated by the magnetic form factor G_M . For neutron form factors there is the additional problem of the lack of a free neutron target, and the (small) relative size of the electric versus the magnetic form factors for small values of Q^2 . With the advent of high duty cycle electron facilities such as ELSA, MAMI, and Jefferson Laboratory far more accurate determinations of the form factors become feasible (ratio method, polarization variables), especially for the neutron form factors (see *e.g.* [2,3]). Recent experiments on electroproduction and eta-photoproduction have yielded valuable new information on transition form factors, in particular on the helicity amplitudes of the $N(1520)D_{13}$ and $N(1535)S_{11}$ resonances [4–6].

The challenge for theoretical calculations is to provide a simultaneous description of both the four elastic form factors and the transition form factors, even if it is only in a phenomenological approach. In this contribution we present such an analysis in the framework of a recently introduced algebraic model of the nucleon [7].

II. ALGEBRAIC MODEL

The algebraic approach provides a unified treatment of various constituent quark models [7], such as harmonic oscillator quark models and collective models. In this paper we employ a collective model of the nucleon in which baryon resonances are interpreted as vibrational and rotational excitations of an oblate top. There are two fundamental vibrations: a breathing mode and a two-dimensional vibrational mode, which are associated with the $N(1440)P_{11}$ Roper resonance and the $N(1710)P_{11}$ resonance, respectively. The negative parity resonances of the second resonance region are interpreted as rotational excitations. Since each vibrational mode has its own characteristic frequency, there is no problem with the mass of the Roper resonance relative to that of the negative parity resonances.

The electromagnetic form factors are obtained by folding with a distribution of the charge and magnetization over the entire volume of the baryon [7]. All calculations are carried out in the Breit frame.

III. ELASTIC FORM FACTORS

In [8] we studied the elastic electromagnetic form factors of the nucleon. These calculations include anomalous magnetic moments for the proton and the neutron, as well as a flavor dependent distribution functions of the charge and magnetization. Supposedly, the anomalous magnetic moments and the flavor dependence arise as effective parameters, since the coupling to the meson cloud surrounding the nucleon was not included explicitly. According to [8] the electric and magnetic form factors of the nucleon, when folded with a distribution of the charge and magnetization, can be expressed in terms of a common intrinsic dipole form factor

$$\begin{aligned} G_E^p(Q^2) &= g(Q^2) , \\ G_E^n(Q^2) &= 0 , \\ G_M^p(Q^2) &= g(Q^2) , \\ G_M^n(Q^2) &= -2g(Q^2)/3 , \end{aligned} \quad (1)$$

with

$$g(Q^2) = \frac{1}{(1 + \gamma Q^2)^2} . \quad (2)$$

Note that the form factors of Eq. (1) do not contain anomalous magnetic moments nor involve flavor dependent distribution functions. In order to study the coupling to the meson cloud we express the electric and magnetic form factors in terms of their isoscalar (S) and isovector (V) components

$$\begin{aligned} G_E^S(Q^2) &= G_E^p(Q^2) + G_E^n(Q^2) = g(Q^2) , \\ G_E^V(Q^2) &= G_E^p(Q^2) - G_E^n(Q^2) = g(Q^2) , \\ G_M^S(Q^2) &= G_M^p(Q^2) + G_M^n(Q^2) = g(Q^2)/3 , \\ G_M^V(Q^2) &= G_M^p(Q^2) - G_M^n(Q^2) = 5g(Q^2)/3 . \end{aligned} \quad (3)$$

A. Meson cloud couplings

The effects of the meson cloud surrounding the nucleon are taken into account by including the coupling to the isoscalar vector mesons ω and ϕ and the isovector vector meson ρ . These contributions are studied phenomenologically by parametrizing the isoscalar and isovector components of the form factors as

$$\begin{aligned} G_E^S(Q^2) &= g(Q^2) \left[\alpha^S + \alpha_\omega \frac{m_\omega^2}{m_\omega^2 + Q^2} + \alpha_\phi \frac{m_\phi^2}{m_\phi^2 + Q^2} \right] , \\ G_E^V(Q^2) &= g(Q^2) \left[\alpha^V + \alpha_\rho \frac{m_\rho^2}{m_\rho^2 + Q^2} \right] , \\ G_M^S(Q^2) &= \frac{1}{3}g(Q^2) \left[\beta^S + \beta_\omega \frac{m_\omega^2}{m_\omega^2 + Q^2} + \beta_\phi \frac{m_\phi^2}{m_\phi^2 + Q^2} \right] , \\ G_M^V(Q^2) &= \frac{5}{3}g(Q^2) \left[\beta^V + \beta_\rho \frac{m_\rho^2}{m_\rho^2 + Q^2} \right] . \end{aligned} \quad (4)$$

The large width of the ρ meson ($\Gamma_\rho = 151$ MeV) is taken into account by making the replacement [9]

$$\frac{m_\rho^2}{m_\rho^2 + Q^2} \rightarrow \frac{m_\rho^2 + 8\Gamma_\rho m_\pi / \pi}{m_\rho^2 + Q^2 + (4m_\pi^2 + Q^2)\Gamma_\rho \alpha(Q^2)/m_\pi} , \quad (5)$$

with

$$\alpha(Q^2) = \frac{2}{\pi} \left[\frac{4m_\pi^2 + Q^2}{Q^2} \right]^{1/2} \ln \left(\frac{\sqrt{4m_\pi^2 + Q^2} + \sqrt{Q^2}}{2m_\pi} \right) . \quad (6)$$

The coefficients $\alpha^{S/V}$ and $\beta^{S/V}$ in Eq. (4) are determined by the electric charges and the magnetic moments of the nucleon, respectively

$$\begin{aligned}\alpha^S &= 1 - \alpha_\omega - \alpha_\phi , \\ \alpha^V &= 1 - \alpha_\rho , \\ \beta^S &= 3(\mu_p + \mu_n) - \beta_\omega - \beta_\phi , \\ \beta^V &= \frac{3}{5}(\mu_p - \mu_n) - \beta_\rho .\end{aligned}\tag{7}$$

For small values of the momentum transfer the form factors are dominated by the meson dynamics and reduce to a monopole form, whereas for large values the modification of dimensional counting laws from perturbative QCD is taken into account by scaling Q^2 with the strong coupling constant [10,11]

$$Q^2 \rightarrow Q^2 \frac{\alpha_s(0)}{\alpha_s(Q^2)} = Q^2 \frac{\ln[(Q^2 + \Lambda_{asy}^2)/\Lambda_{QCD}^2]}{\ln[\Lambda_{asy}^2/\Lambda_{QCD}^2]} .\tag{8}$$

B. Results

In Figs. 1–4 we show a compilation of the most recent data on the electromagnetic form factors of the nucleon. Most of the data points have been obtained by a separation technique which is based on the Rosenbluth formula for the cross section [12]

$$\frac{d\sigma}{d\Omega} = \left(\frac{d\sigma}{d\Omega} \right)_{Mott} \left[\frac{G_E^2(Q^2) + \tau G_M^2(Q^2)}{1 + \tau} + 2\tau G_M^2(Q^2) \tan^2 \frac{\theta}{2} \right] ,\tag{9}$$

with $\tau = Q^2/4M^2$. Although in principle the electric and magnetic form factors can be separated by varying the scattering angle θ , in practice this separation technique is limited to small values of Q^2 only. For large values of Q^2 the measured cross section is dominated by the magnetic form factor, and hence it becomes increasingly difficult to extract the electric form factor. For the neutron form factors there is the additional problem of the lack of a free neutron target, and the (small) relative size of the electric versus the magnetic form factors for small values of Q^2 . In order to overcome these problems to extract the form factors many times the assumption of form factor scaling (which holds for small values of Q^2) is made

$$G_E^p(Q^2) = \frac{G_M^p(Q^2)}{\mu_p} = \frac{G_M^n(Q^2)}{\mu_n} .\tag{10}$$

As a result, especially for the neutron form factors the scattering of data points is at times even larger than the uncertainties quoted by the authors. With the advent of high duty cycle electron facilities such as *e.g.* ELSA, MAMI and Jefferson Laboratory far more accurate determinations of the form factors become feasible, either using coincidence experiments (ratio method) or polarization variables [2,3]. For example, the use of polarization variables makes it possible to extract the ratio of the electric and magnetic form factors from the data.

In the present calculation the coefficients α_M and β_M (with $M = \rho, \omega, \phi$), the scale parameter γ in the dipole form factor $g(Q^2)$ and the Λ 's are determined in a simultaneous fit to all four electromagnetic form factors of the nucleon and the proton and neutron charge radii. The values of the fitted parameters are given in Table I. As usual, the form factors are scaled by the standard dipole fit $F_D = 1/(1 + Q^2/0.71)^2$. The oscillations around the dipole values are attributed to the meson cloud couplings.

The electric form factors, as well as the proton and neutron charge radii (the slope of G_E^p and G_E^n in the origin) are reproduced well. The electric form factor of the neutron is the least known. Unlike for the proton, the Rosenbluth separation of G_E^n from G_M^n for a neutron target is difficult for all values of Q^2 : for small Q^2 because of the small size of G_E^n compared to G_M^n , and for large Q^2 because the magnetic component dominates both the angular dependent and angular independent term in the cross section. For this reason we have included in Fig. 2 only the results obtained from polarization variables [2]. The new data points for G_E^n are significantly larger than those of the Platchkov compilation [15], which in turn leads to a reduction of the cross-over point in the neutron charge distribution from 0.9 fm to 0.7 fm [16]. In the Breit frame, the proton and neutron charge distributions are given by the Fourier transforms of the respective electric form factors

$$\rho_{p/n}(r) = \frac{1}{(2\pi)^3} \int d\vec{q} G_E^{p/n}(q) e^{-i\vec{q}\cdot\vec{r}}. \quad (11)$$

In Figs. 5 and 6 we show the results of our calculations. The neutron charge distribution shows a change in sign at 0.65 fm.

The magnetic form factors show a slight oscillatory behavior around the dipole form. For large values of Q^2 both the proton and the neutron magnetic form factor show a decrease with respect to the dipole. The present calculation is in good agreement with the new measurements of G_M^n at MAMI (Anklin '98 [3]).

In Figs. 7 and 8 we study the form factor scaling relations of Eq. (10). Whereas the ratio of the proton form factors is close to one over the entire range of Q^2 , the ratio of neutron and proton magnetic form factors shows a deviation from form factor scaling. In Figs. 9 and 10 we show two other measures of deviations from form factor scaling. The ratio of neutron and proton Rosenbluth cross sections reduces under the assumption of form factor scaling and for large values of Q^2 to a constant

$$\begin{aligned} \frac{d\sigma_n}{d\Omega} \Big/ \frac{d\sigma_p}{d\Omega} &= \frac{(G_E^n)^2 + \tau(G_M^n)^2 + 2\tau(1+\tau)(G_M^n)^2 \tan^2(\theta_n/2)}{(G_E^p)^2 + \tau(G_M^p)^2 + 2\tau(1+\tau)(G_M^p)^2 \tan^2(\theta_p/2)} \\ &\rightarrow \frac{\tau\mu_n^2 + 2\tau(1+\tau)\mu_n^2 \tan^2(\theta_n/2)}{1 + \tau\mu_p^2 + 2\tau(1+\tau)\mu_p^2 \tan^2(\theta_p/2)} \\ &\rightarrow \frac{\mu_n^2 \tan^2(\theta_n/2)}{\mu_p^2 \tan^2(\theta_p/2)}. \end{aligned} \quad (12)$$

For equal angles ($\theta_n = \theta_p$) this ratio reduces to $\mu_n^2/\mu_p^2 = 0.47$. The transition from the region of low momentum transfer where to good approximation the nucleon form factors satisfy form factor scaling, to the region of high momentum transfer for which the methods of perturbative QCD apply, can be studied by the ratio $Q^2 F_2^p/F_1^p$ of the Dirac (F_1) and Pauli (F_2) form factors

$$\begin{aligned} F_1(Q^2) &= \frac{G_E(Q^2) + \tau G_M(Q^2)}{1 + \tau}, \\ F_2(Q^2) &= \frac{G_M(Q^2) - G_E(Q^2)}{(\mu_p - 1)(1 + \tau)}. \end{aligned} \quad (13)$$

According to dimensional scaling laws the helicity conserving amplitude F_1^p dominates the helicity-flip amplitude F_2^p at high Q^2 , and the ratio $Q^2 F_2^p/F_1^p$ goes to a constant [17]. Under the assumption of form factor scaling and for large values of Q^2 we find

$$\begin{aligned} \frac{Q^2 F_2^p}{F_1^p} &= \frac{Q^2(G_M^p - G_E^p)}{(\mu_p - 1)(G_E^p + \tau G_M^p)} \\ &\rightarrow \frac{Q^2}{1 + \tau\mu_p} \\ &\rightarrow \frac{4M^2}{\mu_p} = 1.26 \text{ (GeV/c)}^2. \end{aligned} \quad (14)$$

In Figs. 9 and 10 both the data and our calculations show a saturation with increasing values of Q^2 . A comparison between the full calculation (solid lines, labeled 'present') and the assumption of form factor scaling (dashed lines, labeled 'scaling') shows that for the ratio of the neutron and proton cross sections there is a large deviation from form factor scaling. For the ratio $Q^2 F_2^p/F_1^p$ the two curves coincide.

For comparison we also show the results of two other calculations: the vector meson dominance model of Iachello, Jackson and Lande [9] (dash-dotted lines, labeled 'IJL'), and a hybrid model (interpolation between vector meson dominance and pQCD) by Gari and Krümpelmann [10] (dash-dashed lines, labeled 'GK'). In comparing the different calculations one has to keep in mind that each one was optimized with the data set of that time (1973 for [9] and 1985 for [10]).

IV. TRANSITION FORM FACTORS

In addition to the elastic form factors, there is currently much interest in the inelastic transition form factors. Recent experiments on eta-photoproduction $\gamma + N \rightarrow N^* + \eta$ have yielded valuable new information on the helicity amplitudes

of the $N(1520)D_{13}$ and $N(1535)S_{11}$ resonances. In an Effective Lagrangian Approach these new experimental results were used to extract model independent ratios of photocouplings [4,5]

$$\begin{aligned} N(1535)S_{11} : \quad & \frac{A_{1/2}^n}{A_{1/2}^p} = -0.84 \pm 0.15 . \\ N(1520)D_{13} : \quad & \frac{A_{3/2}^p}{A_{1/2}^p} = -2.5 \pm 0.2 \pm 0.4 . \end{aligned} \quad (15)$$

These values are in excellent agreement with those of the collective algebraic model, -0.81 and -2.53 , respectively [7] (for the $N(1535)S_{11}$ resonance a mixing angle of $\theta = -38$ degrees was introduced). In Table II we compare these values with some model calculations. Whereas for the ratio $A_{1/2}^n/A_{1/2}^p$ of the $N(1535)S_{11}$ resonance there is little variation between the various theoretical results, for the ratio $A_{3/2}^p/A_{1/2}^p$ of the $N(1520)D_{13}$ resonance there is a large spread in values. Note also the large discrepancy between the photocouplings obtained from electro-photoproduction [25] and the new values determined from eta-photoproduction [4,5,26].

Finally, in Fig. 11 we show the $N(1535)S_{11}$ proton helicity amplitude $A_{1/2}^p$ as a function of Q^2 , for which there exist interesting new data [6] (diamonds). The other points are obtained from a reanalysis of old(er) data, but now using the same values of the resonance parameters for all cases (from a compilation in [6]). The solid curve represents the results of the collective algebraic model of [7], which were obtained by introducing a mixing angle of $\theta = -38$ degrees, but which do not contain the effects of meson-cloud couplings. We find good overall agreement with the data for the entire range of Q^2 values.

V. SUMMARY AND CONCLUSIONS

We presented a simultaneous analysis of the four elastic form factors of the nucleon and the transition form factors in a collective model of baryons, and found in general good agreement with the data.

The elastic electromagnetic form factors of the nucleon were studied for the space-like region $0 \leq Q^2 \leq 10$ (GeV/c)². Whereas for low Q^2 the form factors satisfy to a good approximation form factor scaling, in the region of high Q^2 they exhibit deviations from these simple scaling relations, most notably for the ratio of the neutron and proton magnetic form factors and the neutron and proton cross sections. The deviations of the nucleon form factors at low Q^2 from the dipole form were attributed to couplings to the meson cloud.

For a phenomenological approach (as the present one) a good data set is a prerequisite. Whereas the proton form factors are relatively well known, there is still quite some controversy about the neutron form factors. New measurements of the polarization asymmetry in which the ratio of the electric and magnetic form factor of the neutron is extracted may help to further clarify the experimental situation.

In conclusion, the present analysis of electromagnetic couplings shows that the collective model of baryons provides a good overall description of the available data.

ACKNOWLEDGEMENTS

This work is supported in part by DGAPA-UNAM under project IN101997 and by grant No. 94-00059 from the United States-Israel Binational Science Foundation (BSF), Jerusalem, Israel.

-
- [1] See *e.g.* Baryons '95, Proceedings of the 7th International Conference on the Structure of Baryons, Eds. B.F. Gibson, P.D. Barnes, J.B. McClelland and W. Weise, World Scientific, Singapore, 1996.
 - [2] C.E. Jones-Woodward et al., Phys. Rev. C **44**, R571 (1991); A.K. Thompson et al., Phys. Rev. Lett. **68**, 2901 (1992); M. Meyerhoff et al., Phys. Lett. B **327**, 201 (1994); T. Eden et al., Phys. Rev. C **50**, R1749 (1994); H. Schmieden and P. Grabmayr, proceedings of Baryons '98.
 - [3] H. Gao et al., Phys. Rev. C **50**, R546 (1994); H. Anklin et al., Phys. Lett. B **336**, 313 (1994); E.E.W. Bruins et al., Phys. Rev. Lett. **75**, 21 (1995); H. Anklin et al., Phys. Lett. B **428**, 248 (1998).

- [4] N.C. Mukhopadhyay, J.-F. Zhang and M. Benmerrouche, Phys. Lett. B **364**, 1 (1995).
- [5] N.C. Mukhopadhyay and N. Mathur, Phys. Lett. B **444**, 7 (1998).
- [6] C.S. Armstrong et al., Phys. Rev. D, in press. Preprint nucl-ex/9811001.
- [7] R. Bijker, F. Iachello and A. Leviatan, Ann. Phys. (N.Y.) **236**, 69 (1994).
- [8] R. Bijker, F. Iachello and A. Leviatan, Phys. Rev. C **54**, 1935 (1996).
- [9] F. Iachello, A.D. Jackson and A. Lande, Phys. Lett. B **43**, 191 (1973).
- [10] M. Gari and W. Krümpelmann, Z. Phys. A **322**, 689 (1985); Phys. Lett. B **173**, 10 (1986).
- [11] Z. Dziembowski, H. Holtmann, A. Szczurek and J. Speth, Ann. Phys. (N.Y.) **258**, 1 (1997).
- [12] M.N. Rosenbluth, Phys. Rev. **79**, 615 (1950).
- [13] A.F. Sill et al., Phys. Rev. D **48**, 29 (1993); R.C. Walker et al., Phys. Rev. D **49**, 5671 (1994).
- [14] R.G. Arnold et al., Phys. Rev. Lett. **61**, 806 (1988); S. Rock et al., Phys. Rev. D **46**, 24 (1992); A. Lung et al., Phys. Rev. Lett. **70**, 718 (1993); P. Markowitz et al., Phys. Rev. C **48**, R5 (1993);
- [15] S. Platchkov et al., Nucl. Phys. **A510**, 740 (1990).
- [16] D. Drechsel, in Proceedings of Baryons '98, preprint nucl-th/9811035.
- [17] S.J. Brodsky and G.R. Farrar, Phys. Rev. D **11**, 1309 (1975).
- [18] R.P. Feynman, M. Kislinger and F. Ravndal, Phys. Rev. D **3**, 2706 (1971).
- [19] R. Koniuk and N. Isgur, Phys. Rev. D **21**, 1868 (1980).
- [20] M. Warns, W. Pfeil and H. Rollnik, Phys. Rev. D **42**, 2215 (1990).
- [21] F.E. Close and Z. Li, Phys. Rev. D **42**, 2194 (1990).
- [22] Z. Li and F.E. Close, Phys. Rev. D **42**, 2207 (1990).
- [23] S. Capstick, Phys. Rev. D **46**, 2864 (1992).
- [24] E. Santopinto, F. Iachello and M.M. Giannini, Eur. Phys. J. A **1**, 307 (1998).
- [25] Particle Data Group, Eur. Phys. J. C **3**, 1 (1998).
- [26] L. Tiator, D. Drechsel, G. Knöchlein and C. Bennhold, preprint nucl-th/9902028.

TABLE I. Parameter values.

Parameter	Fit	
γ	0.710	GeV^{-2}
α_ρ	0.371	
α_ω	0.787	
α_ϕ	-0.677	
β_ρ	1.261	
β_ω	1.171	
β_ϕ	-1.056	
Λ_{asy}	1.439	GeV
Λ_{QCD}	0.217	GeV
χ^2	99/82	

TABLE II. Ratios of helicity amplitudes.

	$N(1535)S_{11}$ $A_{1/2}^n/A_{1/2}^p$	$N(1520)D_{13}$ $A_{3/2}^p/A_{1/2}^p$
Feynman et al. [18]	-0.69	-3.21
Koniuk and Isgur [19]	-0.81	-5.57
Warns et al. [20]	-1.06	-9.00
Close and Li [21]	-0.74	-6.55
	-0.65	-4.87
Li and Close [22]	-0.54	-2.50
	-0.56	-2.61
Capstick [23]	-0.83	-8.93
Bijker et al. [7]	-0.81	-2.53
Santopinto et al. [24]	-0.68	-1.55
	-0.67	-1.80
Mukhopadhyay et al. [4,5]	-0.84 ± 0.15	$-2.5 \pm 0.2 \pm 0.4$
PDG [25]	-0.51 ± 0.47	-6.9 ± 2.8
Tiator et al. [26]		-2.1 ± 0.2

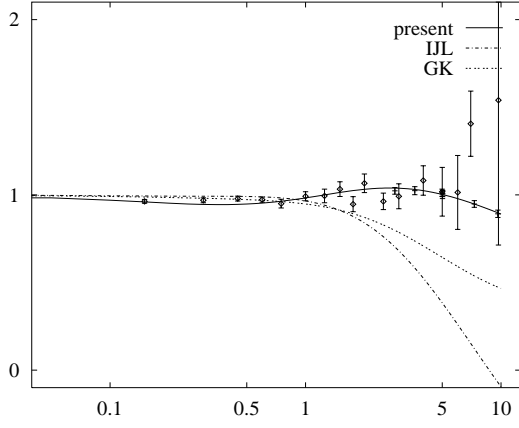


FIG. 1. Proton electric form factor G_E^p/F_D as a function of Q^2 in $(\text{GeV}/c)^2$. The data are taken from [13].

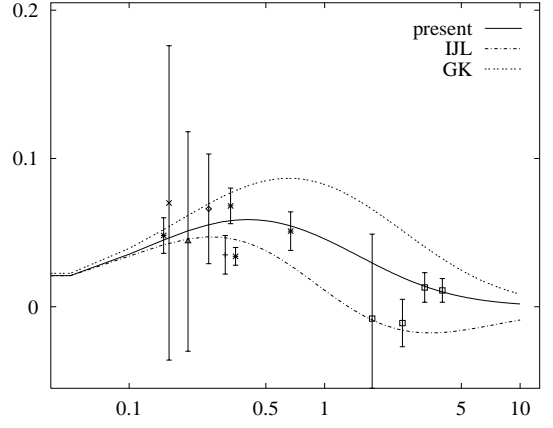


FIG. 2. Neutron electric form factor G_E^n as a function of Q^2 in $(\text{GeV}/c)^2$. The data are taken from [2].

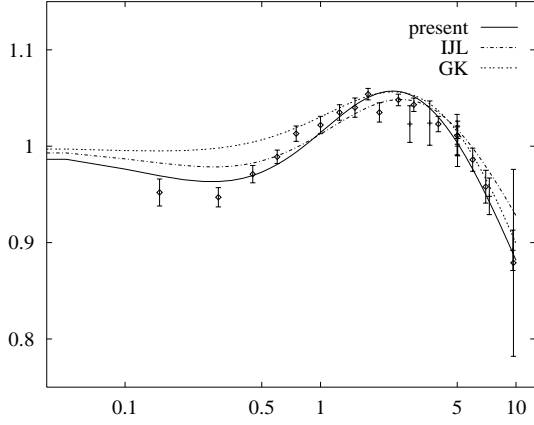


FIG. 3. Proton magnetic form factor $G_M^p/\mu_p F_D$ as a function of Q^2 in $(\text{GeV}/c)^2$. The data are taken from [13].

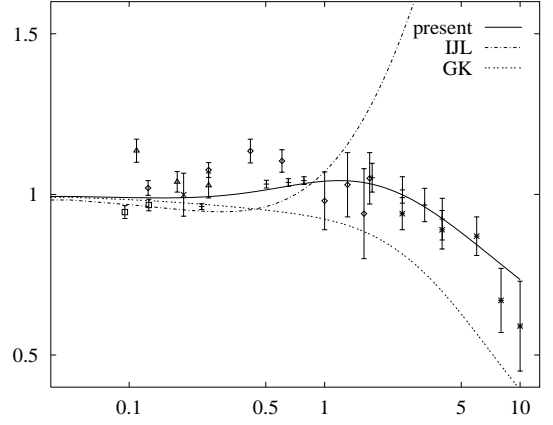


FIG. 4. Neutron magnetic form factor $G_M^n/\mu_n F_D$ as a function of Q^2 in $(\text{GeV}/c)^2$. The data are taken from [14,3].

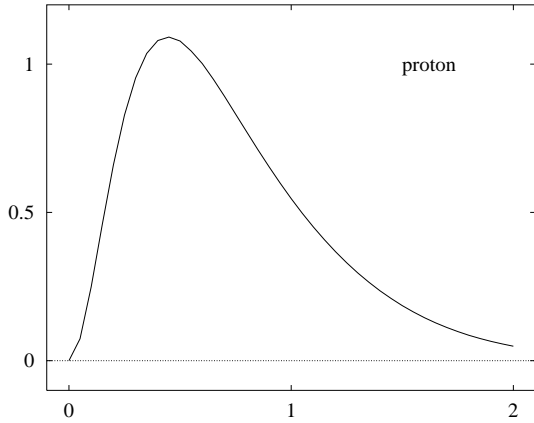


FIG. 5. Charge distribution of the proton $4\pi r^2 \rho_p(r)$ as a function of r in fm.

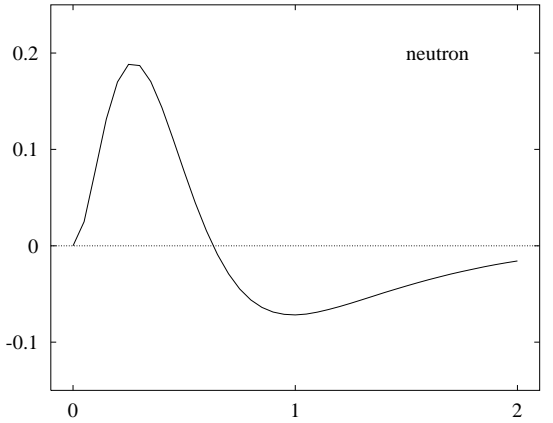


FIG. 6. Charge distribution of the neutron $4\pi r^2 \rho_n(r)$ as a function of r in fm.

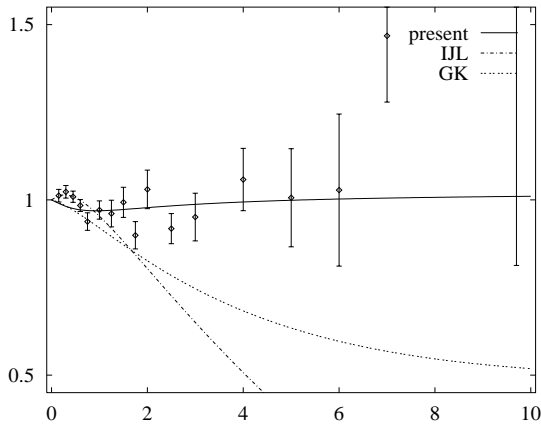


FIG. 7. Ratio of proton form factors $\mu_p G_E^p / G_M^p$ as a function of Q^2 in $(\text{GeV}/c)^2$. The data are taken from Walker et al. [13].

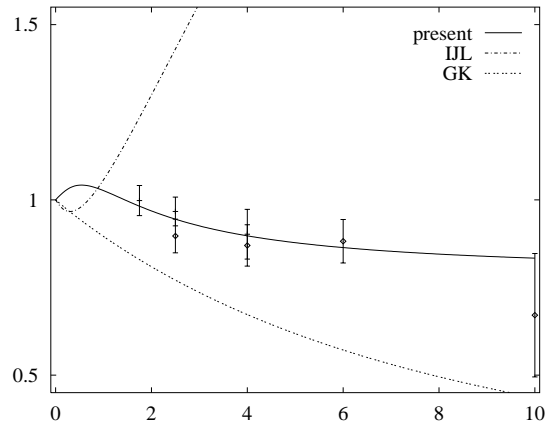


FIG. 8. Ratio of magnetic form factors $\mu_p G_M^n / \mu_n G_M^p$ as a function of Q^2 in $(\text{GeV}/c)^2$. The data are taken from Rock et al. and Lung et al. [14].

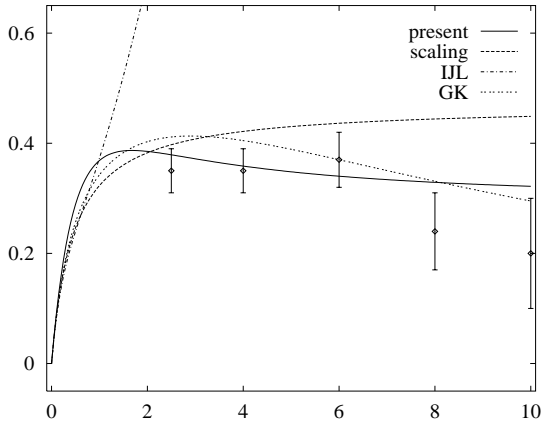


FIG. 9. Ratio of neutron and proton cross section of Eq. (12) as a function of Q^2 in $(\text{GeV}/c)^2$. The data are taken from Rock et al. [14].

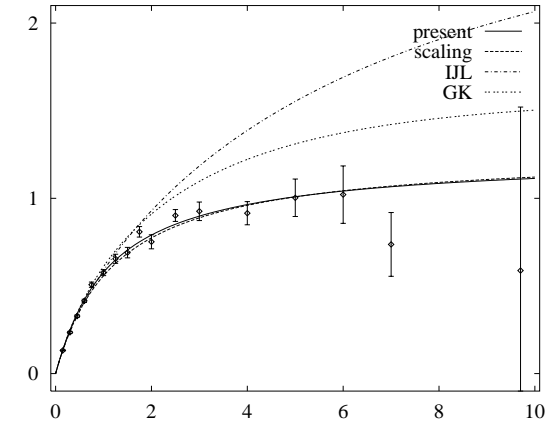


FIG. 10. Ratio of proton Pauli and Dirac form factors of Eq. (14) in $(\text{GeV}/c)^2$ as a function of Q^2 in $(\text{GeV}/c)^2$. The data are taken from Walker et al. [13].

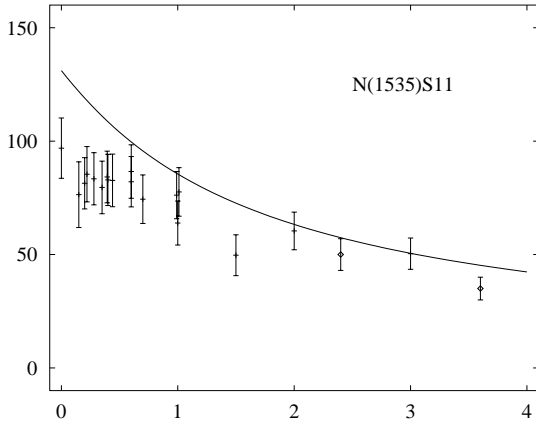


FIG. 11. $N(1535)S_{11}$ proton helicity amplitude in $10^{-3} \text{GeV}^{-1/2}$ as a function of Q^2 in $(\text{GeV}/c)^2$. A factor of $+i$ is suppressed. The data are taken from a compilation in [6].